Evaluation of perpendicular to grain failure of beams caused by concentrated loads of joints, V31 september 2000

van der Put, TACM; Leijten, AJM

Publication date
2000

Document Version
Final published version

2000-2 / V31

EVALUATION OF PERPENDICULAR TO GRAIN FAILURE OF BEAMS CAUSED BY CONCENTRATED LOADS OF JOINTS

september 2000 Dr. ir. T.C.A.M. van der Put/ Dr. ir. A.J.M. Leijten

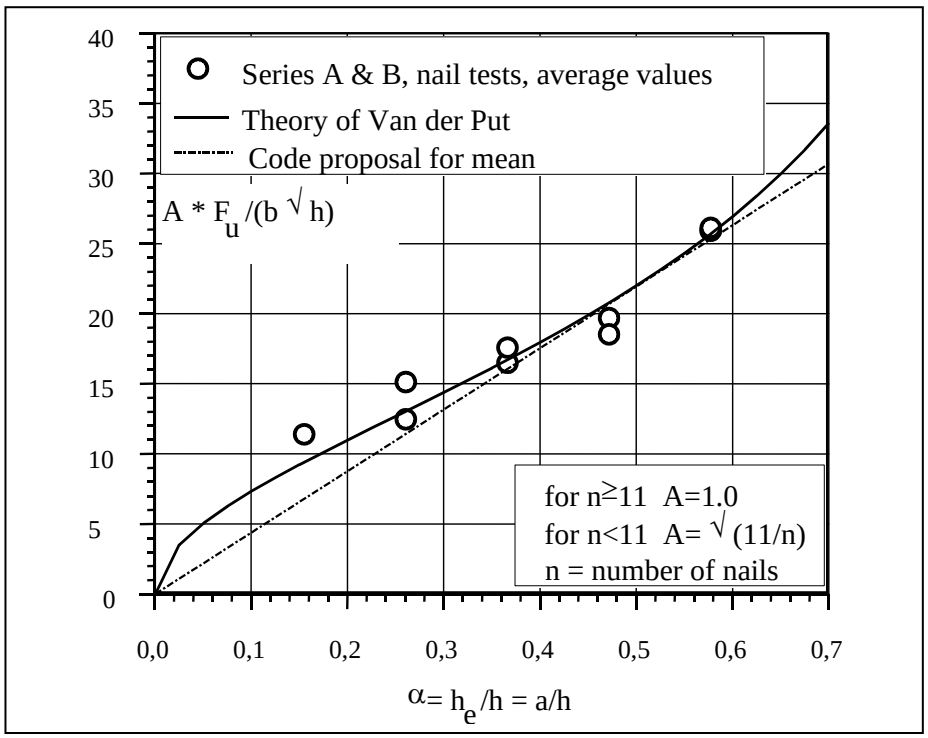

EVALUATION OF PERPENDICULAR TO GRAIN FAILURE OF BEAMS CAUSED BY CONCENTRATED LOADS OF JOINTS

T.A.C.M. van der Put,
Delft Wood Science Foundation
A.J.M. Leijten
Delft University of Technology, the Netherlands

1. Introduction

This paper reviews test data and a fracture mechanical model designed for beams loaded perpendicular to grain by joints, see Figure 5. The aim is to show the capabilities of the model and to give a guideline for Eurocode 5. Splitting of beams loaded perpendicular to the grain by joints, was explained by fracture mechanics by Van der Put, [1] and [2]. An effort is made to make the theory more transparent and to show how well the method explains the test results of [3] and [4].

1.1 Summary

Splitting of beams loaded perpendicular to the grain by joints is explained by fracture mechanics by Van der Put as shown earlier [1] and [2]. Test data of two sources are being considered [3] and [4]. The test data can be divided into four groups. First, the joint is over-designed compared to the splitting strength. Second, the joint start to yield at the moment of splitting. Third, the joint yields followed by hardening and finally splitting of the beam. Fourth, the joint is under-designed and splitting may still occur but probably not sooner than after the elongated holes have damaged the cross-section considerable. An important parameter to distinguish between the cases is the apparent value of $\sqrt{GG_c}$.
In addition a model is presented to predict the capacity of fasteners located near the loaded edge based on the compression strength perpendicular to grain. The theory is given in Appendix II. It is shown that all the available test data can be explained. Simple design equations that derived to be considered by code writers.

2 Fracture mechanic approach

As several modes of crack propagation in two directions are expected to occur the energy approach is convenient to obtain solutions for splitting of beams. As mentioned in the RILEM State of the Art Report on fracture Mechanics (RC-110-TFM, Research Notes 1263, ESPOO 1991) that the energy approach does not show good results, a better concept is derived and verified in [2] and applied for notched beams. This derivation is also given in appendix I. As the behaviour of beams loaded perpendicular to grain by joints is comparable with notched beams the same method is applied, [1] and [2]. The derivation with slightly different constants is given in the following.

3. Fracture of the beam caused by joints.

The same principle and superposition method as given in [2] for notched beams is applied when joints load the beam perpendicular to the grain near the loaded edge. The difference of beam deformation in case of the not-cracked situation and the cracked state is calculated as follows:

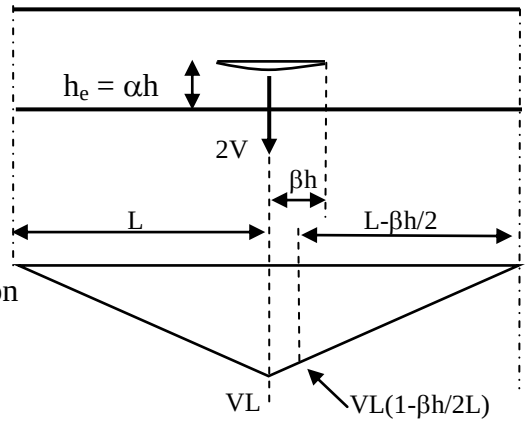

Beam with crack caused by a shear force

Schematic representation of the bending moment diagram

Figure 1: Joint loaded the beam perpendicular at grain at lower part

For a connection as shown in Figure 1 the following applies after a stable split occurs. The crack separated parts divide the bending moment of the initially not-cracked cross-section. A bending moment M is divided into two parts, M_2 is taken by the upper part of the beam (stiffness I_2) and M_1 and the shear force (V) is taken by the lower part (stiffness I_1). Normal forces can be neglected as they are of second order influence. The total crack length is set to $2\lambda=2\beta h$. The rotation φ at the end of crack length $\lambda=\beta h$ can be determined for both part by:

$$\varphi = \frac{M_2\,\lambda}{\mathrm{EI}_2} = \frac{(M - M_1)\,\lambda}{\mathrm{EI}_2} = \frac{M_1\lambda}{\mathrm{EI}_1} + \frac{V\lambda^2}{2\mathrm{EI}_1} \qquad (1)$$

with $M = M_1 + M_2$

being the moment at the end of the crack or:

$$M_1(1+\frac{I_2}{I_1}) = M - \frac{V\lambda I_2}{2I_1} \text{ and } \varphi = \frac{\overline{M}\lambda}{E(I_1+I_2)} \qquad (2)$$

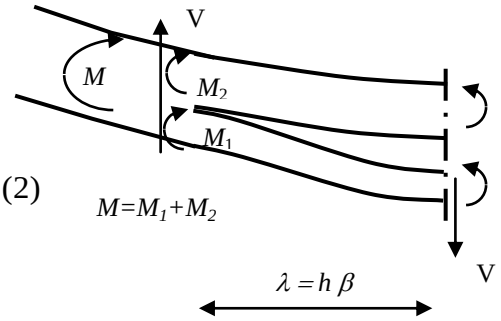

Figure 2: Static of half the crack

where:

$\overline{M} = M + \mathrm{V}\lambda/2$

which is the mean bending moment over half the crack length $\lambda = \beta h$ which corresponds to a bending moment of:

$\overline{M} = VL(1-\beta h/2L)$

The relative deflection consisting of a shear and bending component is:

$\delta = \delta_v + \varphi(L - \beta h/2)$

$$\delta = \frac{1.2}{G}\left(\frac{\beta h}{b\alpha h} - \frac{\beta h}{bh}\right)V + \varphi(L - \beta h/2)$$

and with $\varphi = \dfrac{\overline{M}\lambda}{E(I_1 + I_2)}$ and $\overline{M} = VL(1 - \beta h/2L)$ it follows

$$\delta = \frac{1.2}{G}\left(\frac{\beta h}{b\alpha h} - \frac{\beta h}{bh}\right)V + VL\left(1 - \frac{\beta h}{2L}\right)\frac{\beta h}{E}\left(L - \frac{\beta h}{2}\right)\left(\frac{1}{I_1 + I_2}\right)$$

Furthermore:

$$\frac{\delta}{V} = \frac{1.2}{Gb}\beta\left(\frac{1}{\alpha} - 1\right) + L\left(1 - \frac{\beta h}{2L}\right)\frac{\beta h}{E}\left(L - \frac{\beta h}{2}\right)\left(\frac{1}{I_1 + I_2}\right) \qquad (3)$$

and

$$\frac{\partial \delta}{\partial \beta V} = \frac{1.2}{Gb}\left(\frac{1}{\alpha} - 1\right) + \frac{12\eta^2}{Eb}\left(1 - \frac{\beta}{2\eta}\right)\left(1 - \frac{3\beta}{2\eta}\right)\left(\frac{3\alpha(1-\alpha)}{1 - 3\alpha(1-\alpha)}\right) \qquad (4)$$

Where η is the L/h ratio

Substitution of $\gamma = 2\eta/3 - \beta$ in

$$\left(1 - \frac{\beta}{2\eta}\right)\left(1 - \frac{3\beta}{2\eta}\right) = \left(\frac{\gamma}{\eta}\right)\left(1 + \frac{3\gamma}{4\eta}\right) \approx \frac{\gamma}{\eta}$$

The potential energy of the symmetrical half of the beam is $W = V\,\delta/2$ were δ is the deflection in the middle. When V is constant the increase of the crack length Δx will increase the deflection with $\Delta\delta$. When the loss of potential energy ΔW becomes equal to the energy of the crack formation, crack propagation occurs, with $\Delta x = h\,\Delta\beta$. According to the principle [1] is

$$\int V\,\mathrm{d}\delta = \int G_f bh\,\mathrm{d}\beta = bh\int G_f\,\mathrm{d}\beta = G_{f,m}bh\beta$$

$$\int V\,\mathrm{d}\delta = \int V\frac{\partial \delta}{\partial V}\mathrm{d}V = \frac{\partial \delta}{\partial V}\int \mathrm{d}\left(\frac{V^2}{2}\right) = \frac{\partial \delta}{\partial V}\frac{V_f{}^2}{2}$$

where $\dfrac{\partial \delta}{\partial V} = \dfrac{\delta}{V}$ independent of V

At the constant maximal value of the shear force V fracture occurs when

$$\frac{\partial(\partial\delta/\partial V)}{\partial \beta}\cdot\frac{V_f^2}{2} = \int \frac{\partial G_f}{\partial \beta}\mathrm{d}\beta = \int^{C} dG_f = G_c$$

$$or\ V_f = \sqrt{\frac{2G_c}{\dfrac{\partial(\delta/V)}{\partial \beta}}} \qquad (5)$$

At the start of crack propagation G_f should be high enough to propagate also in width direction. When G_l and G_w are both the energy release rates in length and width direction it follows:

$$G_l bh\Delta\beta + G_w bh\Delta\xi = G_f bh\Delta\beta(1+\frac{G_w}{G_l}\frac{d\xi}{d\beta}) = G_f' bh\Delta\beta$$

Both G's are assumed to be covered by the apparent value of G_f'. Determining for total fracture is the combined mode I and II in length direction, see appendix I.

Substitution of the above in eq.(5) and for small values of β and E/G=18 it follows:

$$\frac{V_f}{b\alpha h} = \frac{\sqrt{GG_c/h}}{\sqrt{0.6\alpha(1-\alpha)+\eta\alpha^3(1-\alpha)\gamma/(1-3\alpha+3\alpha^3)}} \qquad (6)$$

The second term in the denominator appears to have a small influence for small values of α and η in the available test data. Also for increasing (stable) crack extension (or increase of β) the eq.(6) becomes eq.(7) for $\beta \approx 2\eta/3$, or $\gamma \approx 0$ giving an upper limit for failure.

$$\frac{V}{b\alpha h} = \frac{\sqrt{GG_c/h}}{\sqrt{0.6\alpha(1-\alpha)}} \quad or \quad \frac{V_f}{b\sqrt{h}} = \sqrt{GG_c}\sqrt{\frac{\alpha}{0.6(1-\alpha)}} \qquad (7)$$

For higher values of η (L/h ratio of a simply supported beam) not tested in [5], for instance $\eta \geq 5$ the splitting strength will not be determining over bending or shear failure and other failure mechanisms depending on the loading.

4. Failure caused by joints [4]

This chapter comprises a reaction on CIB/W18 paper 32-7-2 [4] to explain the test results. The dowels used can be regarded as rigid dowels as the slenderness ratio was b/d = 4 where b is the middle member thickness.
The configuration of the joint considered in the next chapters is shown in Figure 5.

4.1 Explanation of the test results of paper CIB/W18/32-7-2

It was reported in [4] that in all tests plastic deformation of the wood occurred prior to splitting. Figure 6 of the paper [4] shows plastic deformations from 4 up to 12mm. Obviously, one dowel of 10 mm diameter used as bearing plate is unable to force bending failure of the whole beam. The embedment stresses calculated as F_u/bd are high compared to the compression strength perpendicular to the grain, Table 1. This so-called hardening is due to confined dilatation perpendicular to the grain and depends on the deformation and thus the ability to spread the concentrated load as shown

$$f_s = c\, f_{c.90}\sqrt{L_s/d} \approx f_{c.90}\sqrt{3a/d} \qquad (8)$$

in Figure 3. This can be explained by the equilibrium method of constructing a stress field in the specimen that satisfies the equilibrium and boundary conditions and that nowhere surmounts the failure criterion. As shown in appendix II it can be derived that the bearing strength can be expressed as:

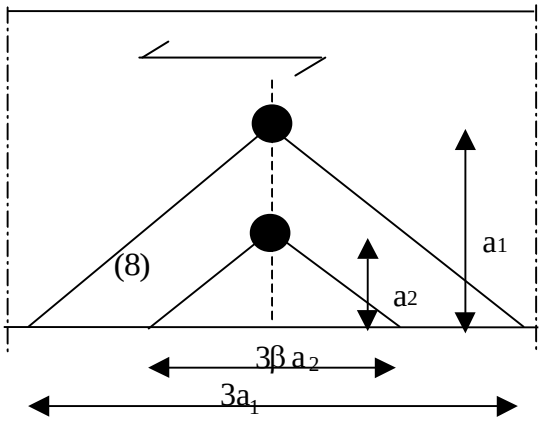

Figure 3: Spreading effect of two dowels

with $c \approx 1$ and a spreading slope 1:1.5 Where $L_s = 3a = 3h_e$ is the spreading length and a the loaded edge distance. In Table 1 the bearing stress f_s and compression stress perpendicular to grain $f_{c.90}$ are derived from the experimental values with eq.(8). In [4] test are performed with a single and with two dowels as shown in Figure 3. According to the theory of Appendix II two dowels in load direction, perpendicular to grain, can build equal resistance only if they have the same spreading surface. The spreading is equal when:

$3a_1 - 3\beta a_2 = 3\beta a_2$ or $\beta a_2 = a_1 / 2$

and both pins have a spreading length of $3a_1/2$

Table 1: Test data of [4]

Specimen	No.of	d	a	Spacing	a/h	$F_u = 2V$	$f_s = F_u/db$	√3a/d	$f_{c.90}$
	test	mm	mm	mm		kN	Mpa		Mpa
	beam: b.h=40.196mm 1 dowel								Eq.(8)
S1-2020	2	10	40	0	0.20	7.6	19.0	3.46	5.5
2025	2	10	50	0	0.26	7.7	19.3	3.87	5
2030	2	10	60	0	0.31	8.3	20.8	4.24	4.9
2035	2	10	70	0	0.36	9.3	23.3	4.58	5.1
2040	2	10	80	0	0.41	10.3	25.8	4.9	5.3
2050	2	10	100	0	0.51	10.6	26.5	5.48	4.8
2060	2	10	120	0	0.61	15.5	38.8	6	6.4
2070	2	24	140	0	0.71	14.7	15.3	4.18	3.7
								mean	**5.1**
	beam: b.h = 40.196 mm 2 dowels							c.o.v	0.15
S2-2035	1	10	70	30	0.36	9.9	12.4	3.24	3.8
2040	1	10	80	30	0.41	12.2	15.3	3.46	4.4
2050	1	10	100	30	0.51	14.7	18.4	3.87	4.8
2060	1	10	120	30	0.61	14.9	18.6	4.24	4.4
2070	2	10	140	30	0.71	13.2	16.5	4.58	3.6
								mean	**4.1**
	beam: b.h = 40.397mm 1 dowels							c.o.v.	0.12
S1-4010	3	10	40	0	0.10	7.2	18	3.46	5.2
4015	2	10	60	0	0.15	7.8	19.5	4.24	4.6
4020	2	10	80	0	0.20	9.4	23.5	4.9	4.8
4025	2	10	100	0	0.25	10.4	26	5.48	4.7
4030	3	10	120	0	0.30	12.9	32.25	6	5.4
4035	1	10	140	0	0.35	12	30	6.48	4.6
4040	2	10/24	160	0	0.40	16.5/18.3	41.3/19.0	6.93/4.47	6.0/4.3
4050	2	10	200	0	0.50	14.8	37	7.75	4.8
4060	2	10/24	240	0	0.60	18.9/20.1	47.3/20.9	8.49/5.48	5.6/3.8
							d=10mm	**mean**	**5.1**
	beam: b.h = 40.397mm 2 dowels							c.o.v.	0.09
S2-4018	1	10	70	30	0.18	9.8	12.3	3.24	3.8
4020	1	10	80	30	0.20	10.6	13.3	3.46	3.8
4030	1	10	120	30	0.30	19.6	24.5	4.24	5.8
4040	1	10	160	30	0.40	17.1	21.4	4.9	4.4
4043	1	10	170	30	0.43	19.6	24.5	5.05	4.9
4050	1	10	200	30	0.50	18.1	22.6	5.48	4.1
4060	1	10	240	30	0.60	24.8	31	6	5.2
4070	1	24	280	30	0.71	35.6	18.5	4.18	4.4
							d=10mm	**mean**	**4.6**
								c.o.v	0.15

S1 – tests with one dowel

S2 – test with two dowels

Mean $f_{c.90}$ values of Table 1.

Series	Per dowel $f_{c.90}$ [Mpa]	Mean
S1-200	5.1	5.1
S1-400	5.1	
S2-200	4.1	4.4
S2-400	4.6	

S1 refers to tests with one dowel,
S2 refers to tests with two dowels.

In tests with two dowels the spacing is small, 3*d*. It appears from this data and also from other investigations that the spacing between the two dowels being less than 4*d* result in reduction of strength by early local failure. This explains the reduction of 4.4/5.1 in the table above. When full bearing is activated at about 1.5*d* deformation only 1.5*d* of spacing is left. The Eurocode5 code should therefore specify 4d as the minimum distance to avoid this effect instead of 3d. The mean strength $f_{c.90}$ = 4.1 MPa for the (three) tests with dowels of 24 mm diameter compared to 5.1 MPa for the 10 mm diameter dowels can be explained by the volume effect.

$$f_{c.90} = f_{c.90,1}\left(\frac{d_1}{d}\right)^n = 5.1\left(\frac{10}{24}\right)^{0.25} = 4.1\,\text{MPa}$$

where n = 3v/1.2 = 2.5v and v is the coefficient of variation of the sample in question. In this case n = 0.25

In Figure 4 it is shown that with eq.(13), derived later, the results with one dowels can be explained. The same appears for the tests with two dowels (no figure given).

It can be concluded that all test results of [4] can be explained by the spreading effect of

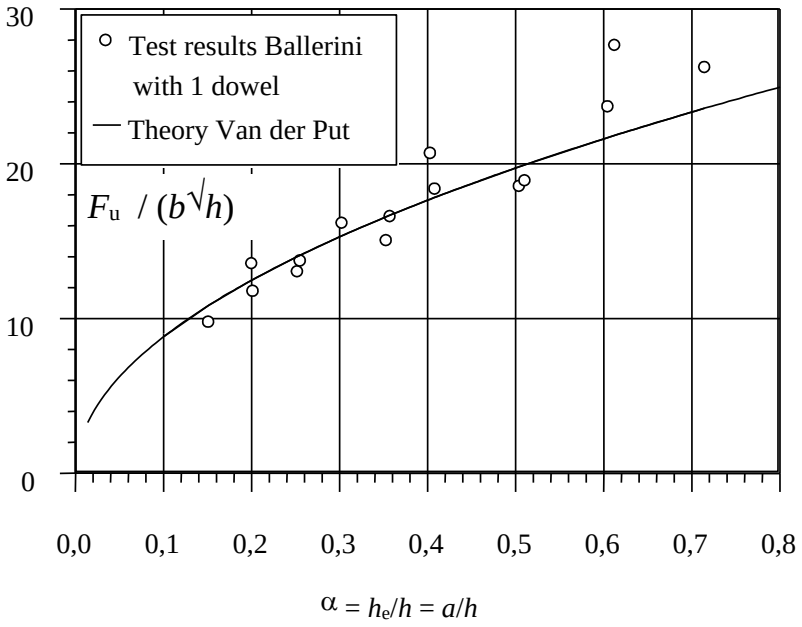

$$\frac{F_u}{b\sqrt{h}} = f_c\sqrt{n.3\alpha d} = 5.1\sqrt{3.10.\alpha} = 27.9\sqrt{\alpha}$$

Figure 4: Explanation of the test data of [4] with eq.(13) with L_s = 3a=3αh

compression perpendicular to grain theory as given above although finally all tests ended by splitting of the beam. It means that actually yielding of the joint started followed by hardening and ending with splitting. As the yielding opens up the cracks at the shear plane of the joint these tests are not particularly suited to study the perpendicular to grain splitting. The upper value for the local strength when the spreading is more than adequate could not be determined as those values were omitted [4].

5 Final state of failure of connections with dowels type fasteners

The previous chapter dealt with a special case of rigid dowels where the spreading of the compression stresses could be considered uniform in beam depth. In this chapter a more general approach is given dependent of dowel slenderness.

After the fastener starts to yield in bending, the resistance of joints with long fasteners still increases, showing only flow or hardening at increasing deformation. As shown in [6] and [7] this is due to the deformed shape of the fastener particularly for nails. The shape of the deformed nail compares well with a logarithmic spiral, where at the final stage the nail is bend over a large angle even up to nearly 90^0. The nails acts as a thin shell showing equilibrium of the embedment stresses with the normal forces in the shank and even yielding of the steel shank may occurs, for instance in the situation shown in Figure 5. In that case only the effective length of the shank takes part in the bearing. The spreading effect mentioned in the previous chapter can no longer be considered in one plane as with rigid dowels. The limited effectiveness of the shank length in spreading should be taken into account as far as it's smaller than half the beam thickness. For slender dowels full bearing across the whole middle beam is possible when sufficient deformation is able to develop. Another fastener type where the effective length is smaller than half the middle member thickness is the punched metal plate. For those cases eq. (8) is transformed into:

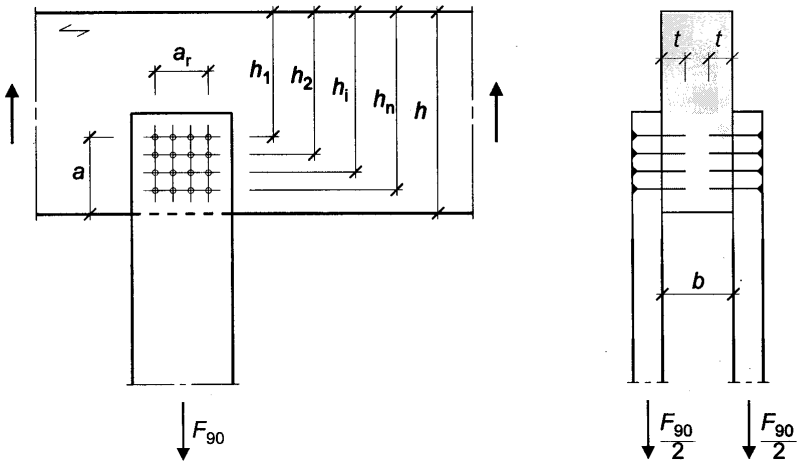

Figure 5: Parameters of a connection perpendicular to grain

$$f_{emb} = f_{c.90}\sqrt{\frac{A_1}{A_0}} = f_{c.90}\sqrt{\frac{L_s\, t}{d\ \lambda d}} \qquad (9)$$

where:

A_1 and A_0 are the spreading and loaded surfaces, respectively.

L_s is the spreading length along the grain

t half the middle member thickness, $b/2$, of the three member joint assuming the loaded edge distance is such that spreading across half the member depth is assured.

λd is the effective length of the fastener

d is the fastener diameter

If the fastener ends in the middle beam as shown in Figure 5. The load per shear plane of the joint per fastener becomes:

$$F/2 = f_{emb} d\, l = f_{emb} d\,(\lambda\, d) = f_{emb} \lambda\, d^2 \qquad (10)$$

Thus total for n fasteners per shear plane

where L_s/n is actually the spreading length per fastener, so with eq.(9) it becomes.

$$F = 2n\, f_{c.90} \sqrt{(L_s t)/(\lambda d^2)}\ \ \lambda\, d^2 \qquad (11)$$

$$F = n\, f_{c.90}\, d \sqrt{2\lambda}\, \sqrt{b\, L_s / n}$$

$$F = f_{c.90}\, d \sqrt{2\lambda} \sqrt{n L_s\, b} = f'_{c,90} d \sqrt{n\, L_s\, b} \qquad (12)$$

When the bearing length is half the member thickness $\lambda\, d = b/2$ as was the case in [4], eq.(12) becomes:

$$F = f_{c.90} b \sqrt{n\, L_s d} \qquad (13)$$

When $\lambda < b/2$, the penetration depth of the fastener ends within the middle member. For long nails with a penetration length of 12d then 3d at the point is needed for clamping, 3d for the anchoring (withdrawal capacity) leaving 6d for bearing. In that case $2\lambda d = 12d$ for two nails in both shear planes of the three member joints and eq.(12) becomes

$$F = f_{c.90} d \sqrt{2\lambda} \sqrt{n\, L_s b} = 3.5\, f_{c.90} d \sqrt{n L_s b} \qquad (14)$$

In eq.(10) to eq.(14) the spreading length $L_s = a_r + 3a$ where a_r is the width of the fastener pattern, see Figure 5.

5.1 Summarising:

The bearing strength of fasteners close to the loaded edge is smaller than the embedment strength as calculated in designing joints by the timber design code. The model that takes this phenomenon into account is as follows:

For nails with penetration depth of more than 12*d*:

$$F = f_{c.90} b \sqrt{n\, L_s d}$$

for $b \leq 12\, d$

$$F = 3.5\, f_{c.90} d \sqrt{n\, L_s d}$$

with

$$L_s = 3a + a_r$$

and

$$f_{c.90} = 5.1 \left(\frac{10}{d} \right)^{0.25}$$

where:

F	is the ultimate load of the middle beam
b	width of the beam (middle member)
n	the number of fasteners/ shear plane
d	fastener diameter, in mm
L_s	is the
a	greatest distance to the loaded edge, Figure 5
a_r	the row length of the fastener pattern

Table 2: TU-Karlsruhe test data No.1: Joint with nails

Type	No.of	d	rows	Col.	$a=\alpha h$	a_r	$F_{u=2V}$	c.o.v.	f_c'	f_c	$\sqrt{GG_c}$	$\eta=L/h$	$F/b\alpha h$
Test	tests		m	N			Mean		Eq(12)	Eq.(13)	Eq.(7)		
NAILS		[mm]			[mm]	[mm]	[kN]		[MPa]	{MPa]	[N/mm$^{1.5}$]		[MPa]
	beam: b.h = 40.180 mm												
L+A1	8	3.8	5	1	28	76	8.25	0.16	12.1	3.7	13.9	2.37	7.37
L7+A2	4	3.8	5	1	47	76	10.94	0.21	13.8	4.3	13.3	2.37	5.82
A3	3	3.8	5	1	66	76	11.93	0.04	13.4	4.2	11.3	2.37	4.52
A4	3	3.8	5	1	85	76	13.40	0.07	13.7	4.2	10.2	2.37	3.94
A5	3	3.8	5	1	104	76	18.90	0.21	17.8	5.5	11.7	2.37	4.54
	beam: b.h = 40.180 mm							**mean**	**14.2**	**4.4**	**12.1**		
L6+B1	4	3.8	5	2	47	76	12.73	0.05	11.4	3.5	15.5	2.37	6.77
B2	3	3.8	5	3	66	76	18.87	0.24	12.2	3.8	17.9	2.37	7.15
B3	3	3.8	5	4	85	76	21.13	0.26	10.8	3.3	16.1	2.37	6.21
B4	3	3.8	5	5	104	76	27.83	0.12	11.8	3.6	17.2	2.37	6.69
	beam: b.h = 40.120 mm							**mean**	**11.6**	**3.6**	**16.7**		
C1	3	3.8	2	1	28	76	9.53	0.12	22.1	6.8	15.3	2.18	8.51
C2	3	3.8	2	1	28	57	8.07	0.05	20.0	6.2	13.0	2.26	7.21
C3	3	3.8	2	1	28	38	6.80	0.02	18.1	5.6	10.9	2.34	6.07
C4	3	3.8	2	1	28	19	6.42	0.12	18.6	5.7	10.3	2.42	5.73
C5	3	3.8	1	1	28	0	6.95	0.20	22.3	6.9	11.2	2.50	6.21
C6	3	8	1	1	28	0	6.05	0.13	13.2	5.8	9.7	2.50	5.40
	beam: b.h = 40.180 mm							**mean**	**19.1**	**6.2**	**11.7**		
L8	1	8	1	1	28	0	5.20	-	11.2	5.0	8.8	2.50	4.64

6 Analyses of TU-Karlsruhe testdata

The test data is given in Tables 2 to 4. The parameters correspond to Figure 5. The ultimate load is given for two shear planes and therefore represent the total load on the middle beam loaded perpendicular to the grain. First a distinction has to be made to what category Series belong. Are the joints "over-designed" or "under-designed" compared to the splitting strength?

In Series B the nails are still loaded to a low level when splitting occurs, indicated by low f_c and f_c' values compared to Series A and C, Table 2. Apparently the joints are "over-designed". Despite the variation in number of nails from 10 to 25 the parameter $\sqrt{GG_c}$ =16.7 N/mm$^{1.5}$ (c.o.v. is 0.07) remains at the same level. The other Series A and C show lower values for $\sqrt{GG_c}$ which is a indication of a different behaviour.

For series C, with long nails, the working or effective length, λd according to eq.(12), of the spiral shape of the deformed nail, becomes larger than half the middle member thickness and thus λd is limited to $b/2$ and eq.(13) applies. From Table 2 it follows that the mean f_c value of Series C is 6.2 N/mm^2 (c.o.v. 0.09). This value can easily be explained by the volume effect. The mean f_c value in [4] was 5.1 for dowels of 10 mm diameter. In Series C the nails are 3.8 mm diameter so:

$$f_{emb} = f_{emb,1}\left(\frac{d_1}{d}\right)^n = 5.1\left(\frac{10}{3.8}\right)^{0.18} = 6.1\,\text{Mpa}$$

In this case the fit indicates n = 0.18.

The influence of the row length a_r is examined by the Series $G_{1.1}$ to $G_{1.4}$, Table 4, having the same geometric parameters except the row length a_r Figure 5. The strength is again governed

by eq.(13). This Series is taken because it can be expected to follow the theory better than Series C where joints are very high loaded at fracture. The influence given in Figure 6 and compared to the provision in the draft German design standard for row length.

Series A and Series V_5 to V_{10} of Table 3, also show a low value for the $\sqrt{GG_c}$ parameter that probably is caused by the number of nails being below the critical number as will be explained later. Confirmation by tests with more nails is necessary to estimate this critical number for Series V.

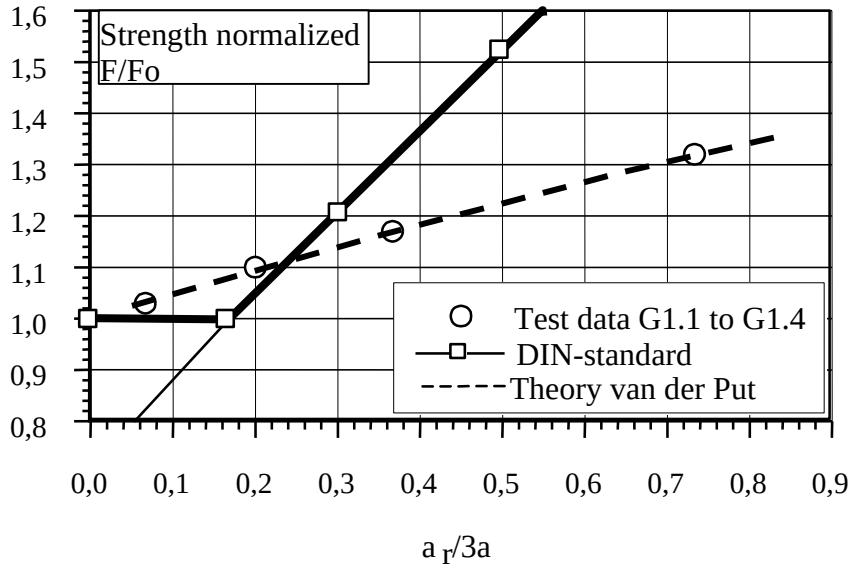

$$y = \frac{F}{F_0} = \sqrt{1 + \frac{a_r}{3a}} \qquad \text{DIN} \quad y = \frac{F}{F_0} = \max\begin{cases} 1.0 \\ \dfrac{0.7 + 1.4\dfrac{a_r}{h}}{1.0} = 0.7 + \dfrac{1.4 a_r}{3a}\dfrac{3a}{h} = 0.7 + \dfrac{a_r}{3a}\dfrac{4.2}{250}\dfrac{100}{} = 0.7 + 1.68\dfrac{a_r}{3a} \end{cases}$$

Figure 6: Influence of row length of fastener pattern a_r

As mentioned earlier low values of $f_c^{'}$ in Table 3 indicate that splitting of the beam is the determining failure mechanism and not the joint. This will be discussed below.

Table 3: TU-Karlsruhe test data No.2

Type	Fastener	No.of	*d*	Rows	col	*a*=α*h*	a_r	F_u =2*V*	*F*/*b*α*h*	$f_c^{'}$	$\sqrt{GG_c}$	η=*L*/*h*	$\sqrt{GG_m}$
	type	Tests		m	n			mean		Eq(12)	Eq.(7)		
			[mm]			[mm]	[mm]	[kN]	[Mpa]	[Mpa]	[N/mm$^{1.5}$]		
	beam:b.h = 100.1200mm												
V5	nails	1	4.2	10	4	300	205	75	2.48	8.44	14.4	1.42	39.7
V10	nails	1	4.2	10	4	600	205	119	1.98	9.96	13.3	1.42	31.7
	beam: b.h = 100.1200 mm								**mean**	**9.2**	**13.9**		
V2	dowels	1	16	3	2	300	205	90	3	6.91	17.5	1.43	48.2
V23	dowels	1	16	3	2	900	205	190	2.11	8.99	12.3	1.43	33.7
V3	dowels	1	16	3	4	300	205	112	3.73	6.08	21.7	1.43	59.9
V9	dowels	1	16	3	6	600	205	179	2.99	5.91	20.1	1.43	48.0
V4	dowels	1	16	2	2	300	205	65	2.17	6.11	12.6	1.37	34.1

	beam: b.h = 100.600 mm								**mean**	**6.8**	**16.8**		
V11/12	dowels	2	16	3	4	300	205	127	4.23	6.89	20.1	0.94	38.9
V13/14	dowels	2	16	3	2	450	205	190	4.22	12.3	17.4	0.94	38.8
V26	dowels	1	16	3	2	450	205	220	4.89	14.2	20.1	1.4	54.9
V24	dowels	1	16	3	2	150	205	70	4.63	6.93	19.0	1.4	54.7
V27	dowels	1	16	3	2	150	205	63	4.17	6.23	17.2	0.44	26.3
V25	dowels	1	16	3	2	300	205	103	3.43	7.91	16.3	1.4	38.5
V28	dowels	1	16	2	2	150	205	56	3.73	6.8	15.3	0.83	32.3
	beam: b.h = 100.1200 mm								**mean**	**8.8**	**17.9**		
V15/16	split-ring	2	65	2	2	300	205	135	4.49		21.3		
V17/18	split-ring	2	65	2	2	450	205	180	4.00		16.5		
V6	split-ring	1	65	1	4	600	0	184	3.06		20.6		
V7	split-ring	1	65	2	2	600	205	117	1.95		13.1		
V8	split-ring	1	65	2	2	300	300	89	2.98		17.3		
V1	split-ring	1	65	2	2	300	205	113	3.76		21.9		
									mean		**18.4**		

In Table 4 all Series show $\sqrt{GG_c}$ values smaller than the critical value of 17 N/mm$^{1.5}$ The strength values F_u are higher than according to the Johanson equations. This also can be

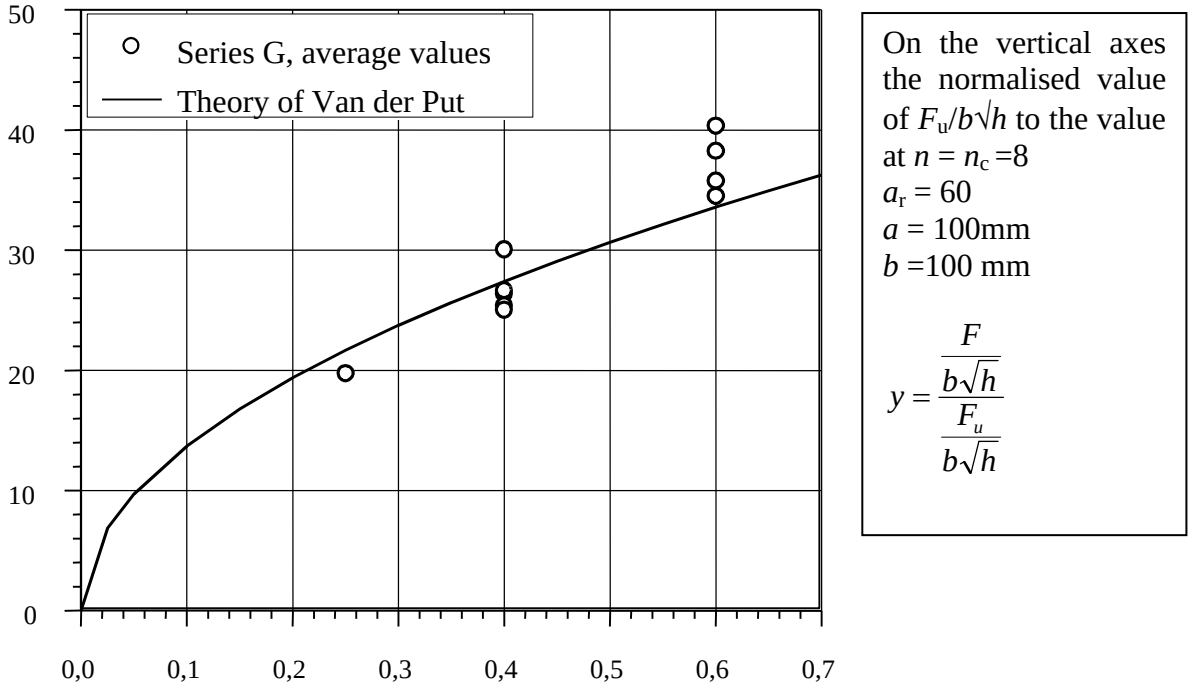

$$y = \frac{F_u}{b\sqrt{h}}\sqrt{\frac{n_c}{n}}\sqrt{\frac{1+60/300}{1+a_r/3a}}\sqrt{\frac{b}{100}} = \frac{F_u}{b\sqrt{h}}\sqrt{\frac{8}{n}}\sqrt{\frac{1.2}{1+a_r/3a}}\sqrt{\frac{b}{100}} = f_c'\sqrt{\frac{d}{b}}\sqrt{d3\alpha 1.2*8} = 43.36\sqrt{\alpha}$$

Figure 7: Failure of the joint, test Series G

expected by the under dimensioned joints and by possible hardening. Series $G_{5.1}$ with only 4 nails per shear plane is 0.85 times as strong as other Series with a comparable beam and 8 nails. For a "small" number of high loaded nails yielding of the nails causes not direct splitting of the beam probably because the crack opening is not yet critical. With a "small"

number of nails splitting becomes finally determining and apparently independent of the number of nails at a value for the apparent parameter $\sqrt{GG_c}$ = 12.2 N/mm$^{1.5}$ as will be discussed in the next chapter. Series G6, joints at the end of a cantilevered beam, has against the rules a nail distance of 7mm or 1.75 *d*, in stead of 4*d*. This obviously reduces the strength, as the hardening effect can't fully develop at the weakest nail.

Table 4: TU-Karlsruhe test data No.3

Type	Fastener	No.of	*d*	rows	col.	$a=\alpha h$	a_r	$F_u=2V$	c.o.v.	$f'c$	$\sqrt{GG_c}$	η	$F/b\alpha h$
	Type	tests		m	n			mean		Eq(12)	Eq.(7)		
			[mm]			[mm]	[mm]	[kN]		[Mpa]	[N/mm$^{1.5}$]		[Mpa]
		beam: b.h = 100.250 mm											
G1.1	Nails*	3	4.0	2	4	100	20	37.3	0.07	18.4	11.2	2.60	3.73
G1.2	Nails*	3	4.0	2	4	100	60	41.7	0.15	19.4	12.5	2.53	4.17
G1.3	Nails*	3	4.0	2	4	100	110	42.9	0.12	18.7	12.9	2.40	4.29
G1.4	Nails*	3	4.0	2	4	100	220	48.0	0.08	18.6	14.4	2.12	4.8
G1.5	Nails*	3	4.0	2	4	150	60	53.0	0.09	20.7	10.6	2.53	3.53
G1.6	Nails*	3	4.0	2	4	150	110	57.6	0.18	21.5	11.5	2.40	3.84
G1.7	Nails*	3	4.0	2	4	150	220	71.1	0.07	24.3	14.2	2.12	4.74
G2.1	Nails*	2	4.0	2	4	100	20	35.7	-	17.6	10.7	2.00	3.57
G2.2	Nails*	2	4.0	2	4	100	60	39.0	-	18.2	11.7	1.50	3.90
		beam: b.h = 80.250 mm							**mean**	**19.7**	**12.2**		
G3.1	Nails*	3	4.0	2	4	100	60	34.9	0.13	18.2	13.1	2.53	4.36
		beam: b.h = 120.250 mm							mean	19.9	11.6		
G3.2	Nails*	3	4.0	2	4	100	60	46.2	0.09	19.6	11.6	2.53	3.85
G3.3	Nails*	3	4.0	2	4	100	60	46.7	0.04	19.8	11.6	2.53	3.89
		beam: b.h = 100.250 mm							**mean**	**19.9**	**11.6**		
G3.4	Nails*	3	6.0	2	4	100	60	44.3	0.05	13.8	13.3	2.53	4.43
		beam: b.h = 100.400 mm											
G4.1	Nails*	3	4.0	2	4	100	60	39.6	0.05	18.4	13.3	1.95	3.95
G4.2	Nails*	3	4.0	2	4	160	60	51.7	0.20	19.7	12.3	1.95	3.23
		beam: b.h = 100.150 mm							**mean**	**19.1**	**12.8**		
G4.3	Nails*	1	4.0	2	4	90	60	47.3	-	23.0	12.2	2.53	5.26
		beam: b.h = 100.250 mm											
G5.1	Nails*	3	4.0	2	2	100	60	35.6	0.22	23.4	10.7	2.52	3.56
G5.2	Nails*	3	4.0	2	2	100	60	33.6	0.18	22.1	10.1	2.52	3.36
G5.3	Nails*	3	4.0	2	4	100	60	42.2	0.09	19.7	12.7	2.52	4.22
									mean	**21.7**	**11.2**		
G6.1	Nails*	2	4.0	2	4	100	20	18.8	-	9.3	11.3	2.48	3.77
G6.2	Nails*	2	4.0	2	4	100	20	23.5	-	11.6	14.1	2.16	4.71
	*) ring shanked nails with steel side members								**mean**	**10.5**	**12.7**		

7. Splitting of the beam

The derived formulas predict stable crack propagation until only shear deformation becomes determining, mode II fracture, resulting in unstable crack propagation. This results in a simple formula given by eq.(7). This equation exactly applies for joints as end supports (and notched beams).

For over-designed, thus "low" loaded joints the splitting strength of the beam, expressed in $\sqrt{GG_c}$, is determining as primary failure mechanism. Series B_2 to B_4 of Table 2 are examples

where the joints are loaded to a low degree and the number of nails have no influence on the splitting capacity, the mean value of $\sqrt{GG_c}$ = 17.1 N/mm$^{1.5}$
However, when the joint is designed less strong the fasteners are higher loaded and yielding may occur at the time of splitting.. For even further under designed joints compared to the splitting strength of the beam the joints may become very high loaded and yielding and/or hardening occur prior to splitting.

Assume that a force V_n leads to the plastic flow of one fastener and with n fasteners the total shear force of eq.(5) becomes $V = n\,V_n$. If V_c is the critical shear force obtained with a critical number of fasteners n_c. That means that splitting of the beam and first flow of the fasteners occur simultaneously, than $V_c = n_c\,V_n$ so $V = n\,V_n / n_c$ and eq.(5) changes into eq.(15). In

$$V_f = \sqrt{\frac{2G_c bh}{\partial\delta/V_c}}\sqrt{\frac{n}{n_c}} \qquad (15)$$

case the number of fasteners is lower than the critical number, until a certain minimum, there is a decrease of the apparent parameter $\sqrt{GG_c}$ in proportion to $\sqrt{(n/n_c)}$. This applies until a minimum value of n because of the low loading of the beam and the relatively small "initial" crack length. For n values below that minimum also splitting is determining independently of the number of fasteners and may occur after the flow or hardening behaviour of the joint when cracks are sufficiently opened.

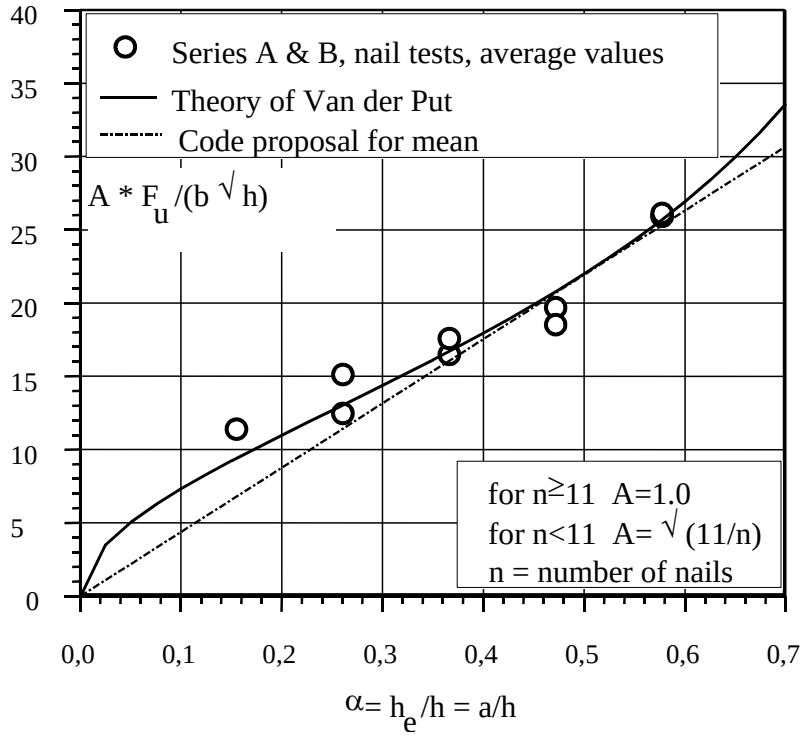

$$y = \frac{F_u}{b\sqrt{h}} = \frac{2V}{b\sqrt{h}} = 22\sqrt{\frac{\alpha}{1-\alpha}}$$

Figure 8: Splitting of the beam, test Series A and B and Equation (7)

For Series B_1, with n = 10 the value of $\sqrt{GG_c}$ = 15.5 N/mm$^{1.5}$ was calculated. The difference 17.0/15.5 = 1.10 equals the factor $\sqrt{n_c}/n$ = $\sqrt{(12.2/10)}$= 1.1 where the critical number of fasteners n_c is taken as 12.2.

The reduction of $\sqrt{GG_c}$ in proportion to $\sqrt{n/n_c}$ goes down to values of $n/n_c \approx 0.5$ to 0.4 as for Series A, where 5 dowel fasteners are used and the mean $\sqrt{GG_c}$ = 12.0 N/mm$^{1.5}$. Taking the mean value of $\sqrt{GG_c}$ = 17.1 N/mm$^{1.5}$ of Series B as a starting point the critical number of fasteners is 10 because 17.1/12= 1.43 = $\sqrt{n_c}/n = \sqrt{10}/5$. The critical number of fasteners n_c in series A and B is almost the same, 10.0 and 12.2 respectively. In Figure 8 the mean test values of the test series A and B are presented together with the theoretical prediction based on eq.(7) and on n_c = 11. For less than five dowels, Series C, first yielding of the nail will occur and hardening will start. However, after some hardening the critical crack length (and width) is formed and splitting will occur. For this reason the joints with 2 fasteners, Series C_1, are after strong hardening as strong as the joints with 5 fasteners, Series L+A_1 and L_7+A_2.
The same reduction effect applies for Series V with dowels, Table 3. For Series V_3, V_{11}/V_{12} and V_9, with n =12 and n = 18 fasteners, respectively, the f_c values are rather low compared to the other tests while the mean of $\sqrt{GG_c} \approx 20.5$ N/mm$^{1.5}$ is high. For the other Series V with n = 4 and 6 the $\sqrt{GG_c}$ is reduced to 12.6 and 16.5, respectively. This leads to a assumed critical number of dowels $n_c \approx 8.6$. The result is presented in Figure 9.

Determining in design of the splitting strength are the joints where the fastener yield and hardening finally results in splitting. This applies for all Series G , Series C and A with mean value for $\sqrt{GG_c}$ of 12.1, 11.8 and 12.0 N/mm$^{1.5}$ respectively.

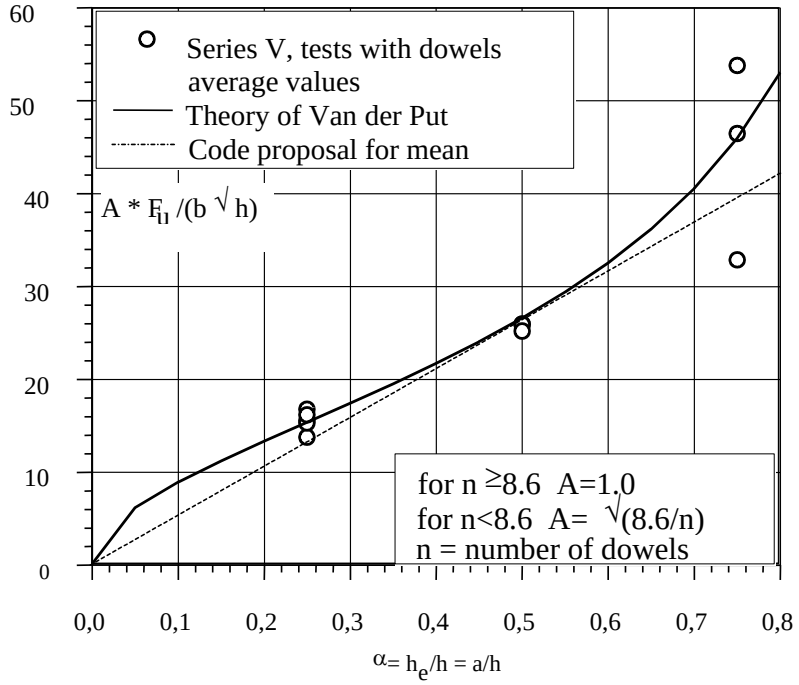

$$y = \frac{F_u}{b\sqrt{h}} = 26.5\sqrt{\frac{\alpha}{1-\alpha}}$$

Figure 9: Splitting of the beam, Series V and Equation (7)

7.1 Design proposals for splitting of the beam

The leading general equation for splitting of the beam is eq.(7), which can be rewritten as:

$$\frac{V_u}{b\sqrt{h}} = \sqrt{\frac{\alpha G G_c}{0.6(1-\alpha)}} = C_1\sqrt{\frac{\alpha}{(1-\alpha)}} \qquad (16)$$

where

$$C_1 = \sqrt{\frac{GG_c}{0.6}}$$

What is the appropriate value for the parameter $\sqrt{GG_c}$. For the test series where the joint do not govern the splitting, Series B, Series V with beam height 1200 and 600 mm (dowels). The weighted mean of $\sqrt{GG_c}$ = 18.5 N/mm$^{1.5}$. This value is about 3 times higher with respect to mode I failure of notched beams indicating a reduced value of the apparent fracture energy of mode II, due to the mixed I-II mode at failure. For the series where the joint were determining, Series A, C and G the weighted mean of factor $\sqrt{GG_c}$ = 12 N/mm$^{1.5}$. The mean lower bound value for C_1 in eq.(16) now becomes $C_1=\sqrt{(GG_c/0.6)}$= 15.5 N/mm$^{1.5}$. Estimation of the characteristic lower bound of C_1= 15.5*2/3 = 10.3 N/mm$^{1.5}$.

Design proposal 1:

The shear capacity of the middle member is:

for $h_e \leq 0.7\ h$

$$\frac{V_u}{b\sqrt{h}} = 10.3\sqrt{\frac{\alpha}{(1-\alpha)}} = 10.3\sqrt{\frac{h_e}{h-h_e}} \qquad (17)$$

To simplify eq.(16) the tangent line can be taken as shown in Figures 8 and 9 by the dotted line. It can be derived that the tangent point is at α = 0.5 and the equation of the dotted line is:

$$\frac{V_u}{b\alpha\sqrt{h}} = 1.7\sqrt{GG_c} \qquad (18)$$

8. Conclusions

- A fracture mechanic model is able to explain the test data related to splitting of the beams loaded perpendicular to grain by joints as given in CIB/W18-22-7-2.

- The fracture mechanics parameter $\sqrt{GG_c}$ plays an important part in the evaluation and interpretation of the test data. The apparent value of $\sqrt{GG_c}$ calculated on the basis of the tests differs for high loaded joints, which show large deformation at splitting and for over-designed low loaded joints, which do not show plastic deformation prior to splitting.
  - When the beam splits and the joints are loaded below their capacity, as in Series B of Table 2, Series V with ring-dowels and joints with more than 6 dowels in Table 3 the apparent value for $\sqrt{GG_c}$ is between 17.1 and 20.5 N/mm$^{1.5}$.
  - When yielding and hardening of the fastener occurs prior to splitting the apparent value for the fracture mechanics parameter becomes $\sqrt{((GG_c)(n/n_c))}$ and changes proportional to $\sqrt{(n/n_c)}$, where n_c is the critical number of fasteners and n the actual number of fasteners. This critical number indicates the boundary between both situations. The lower bound for the apparent $\sqrt{GG_c}$ parameter is probably ≈ 12

$N/mm^{1.5}$ as for test Series A, C and G and probably independent of the number of nails.

- When joints are further under-designed with respect to the splitting strength of the beam the joint can show large plastic flow and hardening too. However, splitting may occur finally when the cross-section is badly damaged by the large elongation of the holes.

- The derived formulas predict a stable crack propagation until the work by shear alone becomes determining leading to a simple formulae, eq.(7).

- Design codes guidelines for the splitting strength capacity of beam exposed to perpendicular to grain loads by joints as shown in Figure 5 are given in eq.(17) and a simplified formula in eq.(19)

  The high embedment stresses of a dowel loaded perpendicular to the grain can be explained by confined dilatation perpendicular to the loading direction as shown in appendix II. Formulae derived from this approach are given in Chapter 5.1

References:

[1] van de Put, T.C.A.M, 1990: Tension perpendicular to grain at notches and joints , CIB/W18/23-10-1, Lisboa, Portugal

[2] van der Put, T.A.C.M., COST 508, workshop2, papers, Bordeaux, April 1992.

[3] Ehlbeck, J. Görlacher, R., Werner, H. CIB/W1822-7-2, meeting 22, Berlin, Germany, sept.1989.

[4] Ballerini, M., 1999, N new set of experimental tests on beams loaded perpendicular to the grain by dowel type joints, CIB/W18, paper 32-7-2, Graz, Austria.

[5] van de Put, T.C.A.M, 1991: Discussion of the failure criterion for combined bending and compression, CIB/W18/24-6-1, Oxford, U.K.

[6] van de Put, T.C.A.M, 1988: Explanation of the embedment strength of particle board, Stevin report, TU-Delft, 25-88-63/09-HSC6 or Ecproject MA1B-0058-NL

[7] van de Put, T.C.A.M, 1982: Betrachtungen zum Bruchmechanismus von nagelverbindungen, Festschrift K.Möhler, Book:Ingenieurholzbau in forschung und Praxis.